Ching-Tai Ng

3D finite element modeling of absorbing regions for guided wave scattering problems in composite materials

GSTF International Journal of Engineering Technology, 2013; 2(1):244-249

http://dx.doi.org/10.5176/2251-3701_2.1.61

3D Finite Element Modeling of Absorbing Regions for Guided Wave Scattering Problems in Composite Materials

Ching-Tai Ng

***Abstract*—This paper presents a three-dimensional (3D) finite element (FE) model of the absorbing regions for guided wave (GW) scattering in composite materials. The model is aimed at providing an efficient and practical numerical modeling technique for analyzing GW propagation and scattering in infinitely long composite structures. The reported study sought to find the optimal configuration of the absorbing regions to not only minimize the wave reflection from boundaries, but also the computational cost. The model with the optimal absorbing regions was then applied to investigate the GW scattering characteristics for different types and sizes of defects in laminated composite beams.**

***Index Terms*—guided wave; absorbing region; finite element; scattering; composite material; damage detection**

I. Introduction

Infrastructure safety has received significant attention in the last decade, with a variety of damage detection methods developed by a number of researchers in an effort to ensure structural safety and reduce maintenance costs [1-3]. Their research suggests that guided wave (GW) offers outstanding detection capabilities, including large area inspection, high sensitivity to most types of damage and high efficiency in detecting small and subsurface defects [4]. The research investigations can be divided into two major areas – scattering characteristics studies [5] and developments of damage detection techniques [6-8].

The use of laminated composite materials has steadily increased in different engineering industries, such as civil, building and aerospace. However, delamination is a serious weakness in structures made with composites as it can cause a reduction of up to 60% in the residual compressive strength of structures [9] and is visually undetectable. The growing use of composite materials, however, has meant that researchers continue to develop methods for detecting hidden delamination in order to ensure structural safety.

The successful development of GW based damage detection techniques requires an understanding of GW propagation and scattering characteristics at defects. Analytical solutions of GW scattering at defects do not exist for laminated composite materials because of their anisotropic nature and multilayer characteristics. On the other hand, a number of studies [10-15] have been carried out using FE simulations to provide improved insight into the scattering phenomena of GWs at different types of defects in laminated composite materials.

Simulations of GWs in structures are computationally expensive as they require an enough number of FE nodes per wavelength of GW to guarantee the accuracy of the simulation results. But the wavelength of GW is usually in the order of millimeters. To improve the computational efficiency of GW simulations, therefore, different FE modeling strategies have been developed for studying the scattering effects. Liu and Quek [16], for example, proposed a non-reflecting boundary for wave propagation in an infinitely long two-dimensional (2D) isotropic plate using a gradually damped artificial boundary; while Drozdz *et al.* [17] suggested a method of modeling GW propagation with a FE method using frequency domain analysis and absorbing regions for isotropic materials. A technique for predicting the far-field scattering behavior of GWs at defects in anisotropic materials developed by Velichko and Wilcox [18] has proved both robust and efficient.

The current study investigates 3D FE modeling of GW propagation with different types of defects in laminated composite beams, as explained in Section II. The effect of using gradually increasing damping in the absorbing region is then discussed in detail in Section III. Section IV demonstrates how the developed 3D FE model can be employed in absorbing regions to study the scattering characteristics of the fundamental anti-symmetric mode (A_0) GWs at different types of defects in laminated composite beams. Finally, conclusions are drawn in Section V.

II. 3D Finite Element Simulations

A. Modeling of guided waves in laminated composite beams

GW propagation and scattering in laminated composite beams is described by a governing equation as a general structural dynamic problem

$$\mathbf{M}\ddot{\mathbf{u}} + \mathbf{C}\dot{\mathbf{u}} + \mathbf{K}\mathbf{u} = \mathbf{P} \tag{1}$$

where $\ddot{\mathbf{u}}$, $\dot{\mathbf{u}}$ and $\mathbf{u}$ are acceleration, velocity and displacement vectors. $\mathbf{M}$, $\mathbf{C}$, $\mathbf{K}$ and $\mathbf{P}$ are the mass matrix, damping matrix, stiffness matrix and external force vector. Commercial FE software ABAQUS/Standard can be used to solve the

Manuscript received April 17, 2013. This work was supported in part by the Australian Research Council under Grant DE130100261.

The author is with the School of Civil, Environmental & Mining Engineering, The University of Adelaide, Adelaide, South Australia, Australia (e-mail: alex.ng@adelaide.edu.au).

DOI: 10.5176/2251-3701_2.1.61

dynamics problems. ABAQUS/Standard employs an implicit FE method using the Newmark integration scheme and the Hilber-Hughes-Taylor method [19].

A $[-45/45/0/90]_S$ laminated composite beam was selected as the specimen for the current study. Each lamina was assumed to be a Cycom® 970/T300 unidirectional carbon/epoxy prepreg tape. The tape was 0.2 mm thick, and the material properties were: Young's modulus $E_1 = 128.75$ GPa, $E_2 = E_3 = 8.35$ GPa; shear modulus $G_{12} = G_{13} = 4.47$ GPa, $G_{23} = 2.90$ GPa; Poisson's ratio $\nu_{12} = \nu_{13} = 0.33$, $\nu_{23} = 0.44$. The density was 1517 kg/m^3. The fiber volume fraction was 0.55. Each lamina was modeled by 8-noded, 3D reduced integration solid brick elements (C3D8R) with hourglass control; and orthotropic material could be assumed, given the material properties of the prepreg tape.

The key parameters of the laminated composite beam were beam length L = 200 mm; width b = 4.0 mm; and height h = 1.6 mm (Fig. 1).

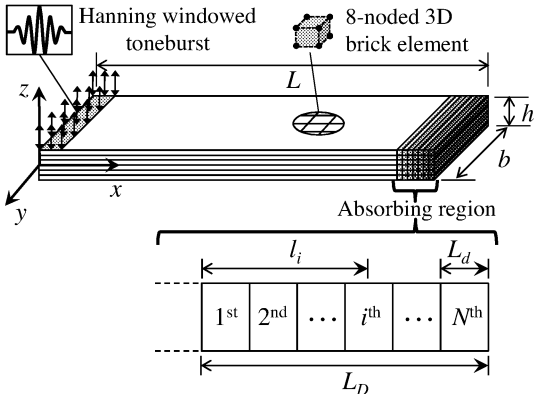

Fig. 1. Schematic diagram of the 3D FE laminated composite beam model

The excitation signal was a 200 kHz narrow-band eight-cycle sinusoidal toneburst pulse modulated by a Hanning window. The A_0 GW was generated by applying the out-of-plane displacement to the nodes in the rectangular area at the beam end as shown in Fig. 1. The A_0 GW at particular locations was obtained by monitoring the out-of-plane displacement of nodes located at the mid-thickness of the laminated composite beam. This ensured that only the A_0 GW was detected since the S_0 and fundamental shear horizontal (SH_0) GW exhibit zero out-of-plane displacement of the nodes located at mid-thickness. The phase velocity, group velocity and wavelength of the excited A_0 GW were 1529.19 m/s, 1259.79 m/s and 6.30 mm. The in-plane dimension of the solid brick elements was 0.4×0.4 mm^2 and the thickness was 0.2 mm. This guaranteed that there were at least 16 FE nodes per wavelength to ensure the accuracy of the simulation results.

The out-of-plane displacements were measured at x = 50 mm, 70 mm, 90 mm, 110 mm and 130 mm; with y = -2.0 mm and z = 0 mm. The FE calculated group velocity (1501.42 m/s) was close to the velocity (1529.19 m/s) calculated by the first order shear deformation theory with coupling between axial-flexural-shear motion.

Two types of damage – notches and delaminations – were considered in the current study. The notches were created by removing elements from the FE model. Delaminations across the full width of the laminated composite beams were modeled by creating duplicate nodes at the delamination interface. Therefore, the coinciding nodes in the delaminated region had a separate identity. Similar modeling techniques were employed in [11,13] and there was good agreement between the FE simulation results and experimental measurements.

B. Modeling of absorbing regions using gradually increased damping

Gradually increased damping can be used to model the absorbing regions for the boundaries of GWs in laminated composite beams. Rayleigh damping, which is a combination of mass- and stiffness-proportional damping, was used in the current study to form the damping matrix $\mathbf{C}$ in (1) as

$$\mathbf{C} = \alpha\mathbf{M} + \beta\mathbf{K} \tag{2}$$

where α and β are Rayleigh coefficients used for damping in the lower and higher frequencies, respectively. For GW problems, damping layers with gradually increasing values of β are used to construct the absorbing regions. As shown in Fig. 1, the value of β_i at the i-th damping layer in the absorbing region can be estimated by [20] as

$$\beta_i = 2\pi f \left(\frac{l_i}{L_D} \right)^2 \quad \text{for } i = 1,...,N \tag{3}$$

where l_i is the distance from the centre of the i-th damping layer to the starting boundary of the absorbing region, as shown in Fig. 1. L_D is the total length of the absorbing region. N is the total number of damping layers in the absorbing region. f (in Hz) is the central frequency of the excited GWs. $L_d = L_D / N$ is the length of each individual damping layer. As indicated in (3) the value of β_i is gradually increased from β_1 to β_N. Assuming the total length of the absorbing region L_D is not fixed, there are fundamentally two parameters N and L_d, controlling the configuration of the absorbing region. It is obvious that the larger the values of N and L_d the larger the size of the FE model, increasing the computational cost of the simulations.

Theoretically, there is a global optimal configuration of the absorbing region that can simultaneously minimize the wave reflected from the boundaries and the computational cost of the simulations. However, the focus of the current study was not to determine the global optimal configuration of the absorbing region. In this study, L_d was assumed to be 0.8 mm in order to determine the optimal value of N that minimizes the wave reflected from the beam end.

III. VALIDATION OF THE ABSORBING REGIONS

A. Optimal value of N for L_d = 0.8 mm

A number of simulations were carried out to determine the optimal value of N. It was assumed for 24 cases that N = 2 to 25. The values of β_i for each case are shown in Fig. 2a, and each curve in Fig. 2a represents one FE simulation. The out-of-plane displacements were monitored at x = 140 mm, y = -2.0 mm and z = 0 mm.

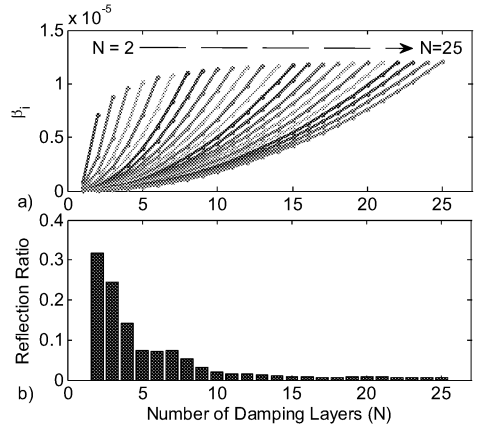

Fig. 2. (a) Values of stiffness-proportional damping and (b) corresponding reflection ratios for different N

Fig. 2a shows the β_i for N values from 2 to 25. A series of parametric studies was conducted using β_i to determine the configuration of the absorbing region that could minimize the wave reflected from the boundaries. The absorbing region was then employed in the FE model developed in Section II, with the out-of-plane displacements monitored at x = 140 mm, y = -2.0 mm and z = 0 mm, the latter of which was 60 mm from the beam end.

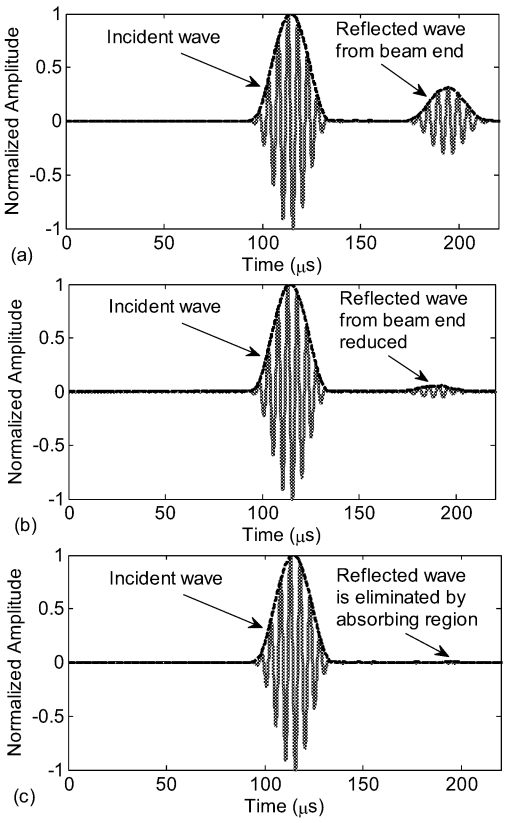

Fig. 3. Normalized ampltiude of guided wave at location x = 140 mm, y = –2.0 mm and z = 0 mm for L_d = 0.8 mm, and (a) N = 2, (b) N = 8 and (c) N = 17. (solid lines: normalized wave signal, dashed lines: normalized wave envelopes calculated by the Hilbert transform)

Figs. 3a, 3b and 3c show the calculated out-of-plane displacements at the monitoring locations for the models with N = 2, 8 and 17, respectively. All calculated out-of-plane displacements were normalized with respect to their maximum displacements at the monitoring location, and hence, the maximum amplitude is equal to 1. The normalized signals and the wave envelopes calculated by the Hilbert transform [3] are indicated as solid and dashed lines, respectively, in Fig. 3.

Fig. 3a shows that the reflection ratio of the wave amplitude reflected from the beam end is reduced to 0.3172 by the absorbing region for which N = 2. The reflection ratio is the ratio of the incident wave amplitude to the reflected wave amplitude at the monitoring location. Fig. 3b shows that the reflection ratio can be further reduced to 0.0521 for the absorbing region for which N = 8. Fig. 3c shows that the reflection ratio for the absorbing region for which N = 17 exhibited the best performance. The figure shows that the amplitude of the wave reflected from the beam end is almost completely eliminated by the absorbing region.

Fig. 2b shows the calculated reflection ratio of the GW from the beam end for the absorbing layer with different values of N. The figure indicates that the reflection ratio is minimized at N = 17, at which point, the reflection ratio is only 0.0066. Therefore, the absorbing region for which N = 17 and L_d = 0.8 mm was selected to investigate the GW scattering characteristics at defects in the laminated composite beam.

IV. Guided Wave Scattering Analysis

As shown in Fig. 4, the absorbing regions for which N = 17 and L_d = 0.8 mm are applied to both sides of the laminated composite beam in order to avoid wave reflection from the beam ends. The configuration of the efficient scattering model is shown in Fig. 4. The total length of each absorbing region at each beam end is 13.6 mm. As shown in Fig. 4, the measured out-of-plane displacements at monitoring points 1 and 2 are reflected and transmitted waves from the defects, respectively.

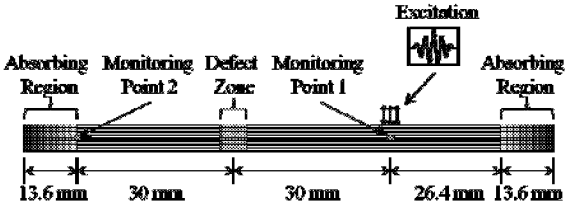

Fig. 4. Schmatic of the 3D finite element scattering model

A. *Effect of notches with different depths*

Once the absorbing regions were validated, notch damage was investigated. As discussed in Section IIA, the notches are modeled by removing elements from the model. Fig. 5 shows four typical contour snapshots of the FE simulated out-of-plane displacement for A_0 GW in the laminated composite beam with a notch. The first and second snapshots in Fig. 5 show that the A_0 GW is generated at monitoring point 1 and then propagates to the notch at the left hand side and the absorbing region at the right beam end.

As shown in the third snapshot, the A_0 GW interacts with the notch, which induces a transmitted and reflected wave in the laminated composite beam. Simultaneously, the excited A_0 GW is absorbed by the absorbing region at the left beam end. The induced transmitted and reflected waves then propagate and

reach monitoring points 1 and 2, as shown in the forth snapshot in Fig. 5.

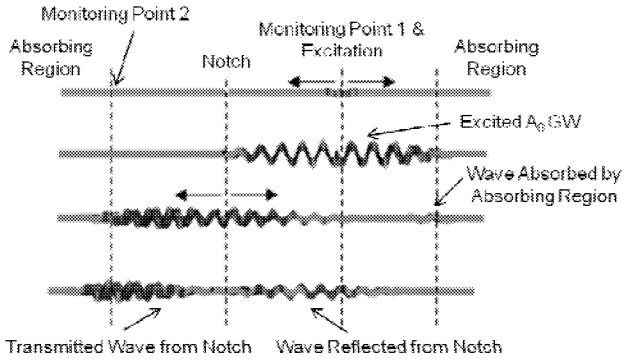

Fig. 5. Typical contour snapshots of FE simulated out-of-plane dispalcment for a A_0 guided wave in the laminated composite beam with a notch

A series of FE simulations was performed, in which each simulation dealt with a notch of a different size. The effect of varying notch depths from 0.2 mm to 1.2 mm in 0.2 mm step increments was first investigated. The width of all the notches was 0.8 mm. Fig. 6 shows the envelopes of the reflected waves calculated at monitoring point 1. As the absorbing regions are used to eliminate the reflected waves from the beam ends, the signals in the figure only contain the incident wave and the wave reflected from the notches. In Fig. 6 the first wave peak represents the incident wave and the second represents the reflected wave from the notches.

In the present study the maximum amplitude of the reflected waves from the notches was a focus of the investigation. The reflected wave amplitude increased with the increase in notch depth. However, the reflected wave amplitude of the notch 1.4 mm in depth proved to be slightly less than that of the notch 1.2 mm deep. This phenomenon is consistent with the findings in [21], in which the reflected wave amplitude had a similar change with the increase in notch depth.

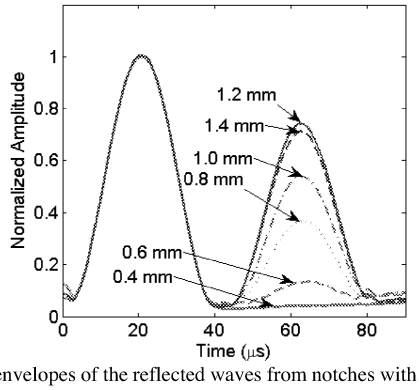

Fig. 6. Wave envelopes of the reflected waves from notches with 0.8 mm width and varying depths

Fig. 7 shows the envelopes of the transmitted waves at monitoring point 2. In contrast with Fig. 6, the signals shown in Fig. 7 only contain one wave pack because monitoring point 2 is located after the notches, causing the incident wave and the wave induced by the notch to overlap. As shown in Fig. 7, the amplitude of the transmitted wave envelopes decreases with the notch depth as a result of the scattering of energy that converts transmitted waves into reflected waves at the notches.

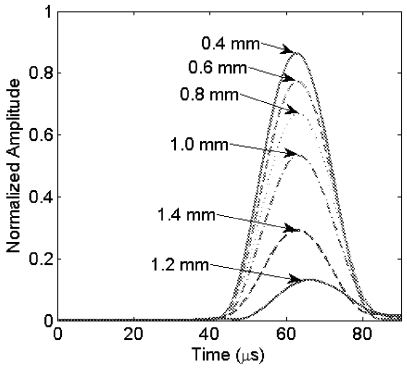

Fig. 7. Wave envelopes of the transmitted waves from notches 0.8 mm wide of varying depths

B. Effect of notches with different widths

Notches with widths varying from 0.4 to 2.4 mm with 0.4 mm step increments were also investigated, as described in this subsection. The depth of all notches was maintained at 0.8 mm. Figs. 10 and 11 show the envelopes of the reflected and transmitted waves calculated at monitoring points 1 and 2, respectively. In contrast to the results of the notches of varying depths in Section IVA, the reflected and transmitted wave amplitude from the notches does not increase or decrease linearly in relation to notch width. The amplitude of the waves reflected and transmitted from the notches follows either a sinusoidal or cosinusoidal pattern according to the width of the notch [21].

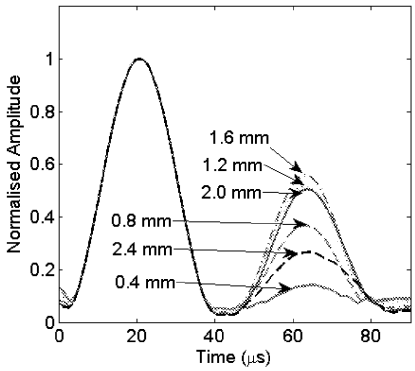

Fig. 8. Wave envelopes of the waves reflected from notches 0.8 mm deep and of varying widths

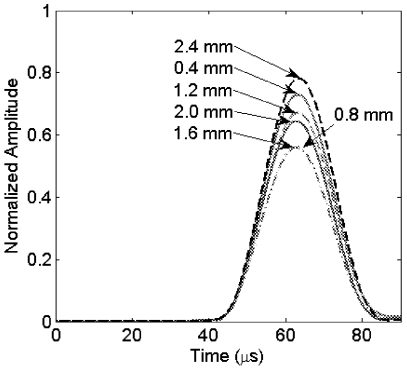

Fig. 9.Wave envelopes of the waves transmitted from notches 0.8 mm deep and of varying widths

C. *Effect of delaminations with different lengths*

Investigations of delaminations of different lengths are described in this subsection. Figs. 10 and 11 show the calculated envelopes of reflected and transmitted waves at monitoring points 1 and 2, respectively. The delaminations were located between the 4th and 5th lamina, which are mid-plane ($z = 0$) of the laminated composite beam. The wave envelope amplitudes were normalized so that the amplitude of the incident wave at monitoring point 1 equaled 1. As shown in Fig. 10, the widths of the reflected wave envelopes for 8 and 10 mm long delaminations are wider than those for 4 and 6 mm delaminations. These results reflect the fact that the wavelength of the incident wave is shorter than the 8 and 10 mm long delaminations, and therefore, multiple wave reflections can occur, increasing the width of the reflected waves.

The amplitude of the waves reflected from the delaminations was usually smaller than the amplitude of the waves reflected from the notches. Fig. 11 shows the amplitude of the waves transmitted from the delaminations. As shown in Fig. 11, the minimum transmitted wave amplitude is 75% of the incident wave amplitude at monitoring point 1 (Fig. 10). The change in the amplitude of the transmitted wave is smaller than the change in the amplitude of the wave emanating from the notches (Figs. 8 and 9). However, the transmitted wave is still considered sensitive for damage detection.

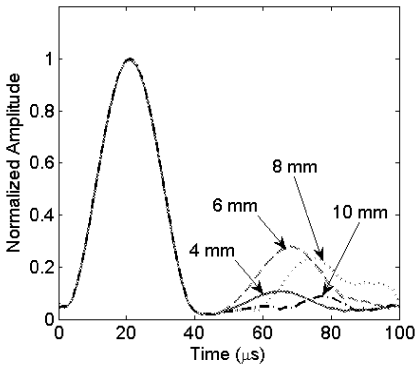

Fig. 10. Wave envelopes of the reflected waves from delaminations of varying lengths

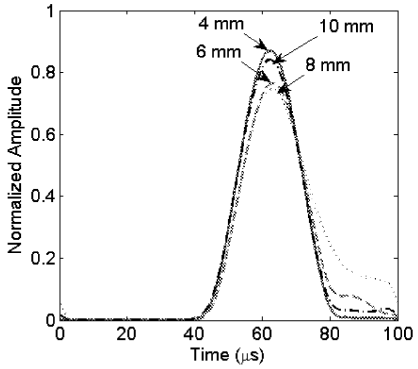

Fig. 11. Wave envelopes of the transmitted waves from delaminations of varying lengths

D. *Effect of delaminations at different through-thickness locations*

It is obvious that the delaminations at different through-thickness locations have different effects on the A_0 GW scattering characteristics. This subsection further investigates this phenomenon by considering 8 mm long delaminations located between the 4th and 5th, 3rd and 4th, 2nd and 3rd, and 1st and 2nd lamina of the composite beam. The results of the reflected and transmitted wave amplitudes are shown in Figs. 12 and 13, respectively. These results are labeled L4-5, L3-4, L2-3 and L1-2. Although all the delaminations have the same length, the reflected and transmitted wave amplitudes are different for the delaminations located between the 4th and 5th, 3rd and 4th, 2nd and 3rd, and 1st and 2nd lamina. This is mainly due to the mode conversion effect, in which part of the reflected and transmitted A_0 wave energy is converted to other GW modes.

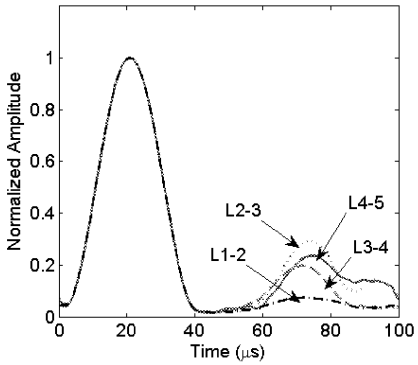

Fig. 12. Wave envelopes of the reflected waves from 8 mm long delaminations at different through-locations

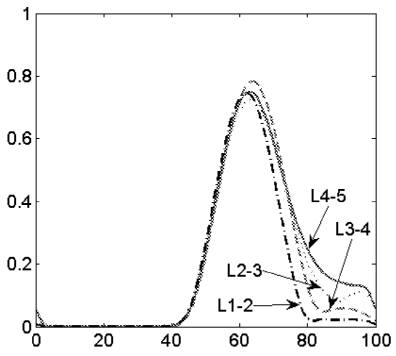

Fig. 13. Wave envelopes of the transmitted waves from 8 mm long delaminations at different through-thickness locations

V. Conclusion

The current study has demonstrated the use of gradually increasing damping to construct the absorbing regions for boundaries of GW problems in composite materials, thereby reducing the size of the FE models and the computational cost of the simulations. The 3D FE method together with the developed absorbing regions were employed in an investigation of the scattering characteristics of the A_0 GW at notches and delaminations in laminated composite beams. A series of case studies was used to investigate the characteristics of the waves reflected and transmitted from these defects. Notches with different depths and widths, and delaminations of varying length and at different through-thickness locations were also investigated. The results of this study provide improved insight into the scattering phenomena of A_0 GW at defects in composite materials, insight which is essential to further advance the development of GW damage detection techniques.

ACKNOWLEDGMENT

The author thanks Mr. Yang Yi and Ms. Yueyang Chen, who have undertaken the numerical simulations in this paper as part of their undergraduate theses. This research is part of an ongoing structural health monitoring program at The University of Adelaide.

REFERENCES

[1] W. J. Stazewski, C. Boller and G. Tomlinson, "Health Monitoring of Aerospace Structures: Smart Sensor Technologies and Signal Processing," West Sussex, UK: Wiley, 2004.

[2] H. F. Lam, C. T. Ng and A. Y. T. Leung, "Multcrack detection on semirigidly connected beams utilizing dynmaic data," *J. Eng. Mech. ASCE*, vol.134, pp.90–99, 2008.

[3] C. T. Ng and M. Veidt, "A Lamb-wave-absed techniuqe for damage detection in compoiste laminates," *Smart Mater. Struct.*, vol. 18(074006), pp.1–12, 2009.

[4] J. L. Rose, "A baseline and vision of ultrasonic guided wave inspection potential," *J. Pressure Vessel Technol.*, vol 124, pp.273–282, 2002.

[5] M. J. S. Lowe, P. Cawley, J. Y. Kao and O. Diligent, "The low frequency reflecion characteristics of the fundamental antisymmetric lamb wave A_0 from a rectangular notch in a plate," *J. Acoust. Soc. Am.*, vol. 112, pp.2612-2622, 2002.

[6] M. Veidt, C. T. Ng and T. Wattingeer, "Imaging laminar damage in plate using Lamb wave beamforming," *Adv. Mater. Res.*, vol. 33, pp.293–301, 2009.

[7] C. T. Ng, M. Veidt and H. F. Lam, "Guided wave damage characterisation in beams utilising probabilistic optimisation," *Eng. Struct.*, vol. 31, pp.2842–2850, 2009.

[8] C. T. Ng, M. Veidt and N. Rajic, "Integrated piezoceramic transdcuers for imaging damage in compsite lamiantes," *Proc. of SPIE*, vol. 7493(74932M), pp.1–8, 2009.

[9] G. A. O. Davies and R. Olsson, "Impact on composite structures," *The Aeron. J.*, vol. 108, pp.541–563, 2004.

[10] T. Hayashi and K. Kawashima, "Multiple reflections of Lamb waves at a delamination," *Ultrasonics*, vol. 40, pp.193–197, 2002.

[11] C. T. Ng and M. Veidt, "Scattering analysis of fundamental anti-symmetric Lamb wave at delaminations in composite laminates," *Aust. J. Mech. Eng.*, vol. 8, pp. 197–205, 2011.

[12] M. Veidt and C. T. Ng, "Influnece of stacking sequence on scattering characteriestics of the fundamental anti-symmetric Lamb wvae at through holes in composite laminates," *J. Acoust. Soc. Am.*, vol. 129, pp.1280–1287, 2011.

[13] C. T. Ng and M. Veidt, "Scattering of the fundamental anti-symmetric Lamb wave at delaminations in composite laminates," *J. Acoust. Soc. Am.*, vol. 129, pp.1288–1296, 2011.

[14] C. T. Ng and M. Veidt, "Scattering characteristics of Lamb waves from debondings at structural features in composite laminates," *J. Acoust. Soc. Am.*, vol. 132, pp.115–123, 2012.

[15] C. T. Ng, M. Veidt, L. R. F. Rose and C. H. Wang, "Analytical and finite elmeent prediction of Lamb wave scattering at delaminations in quasi-isotropic composite laminates," *J. Sound and Vib.*, vol. 331, pp.4870–4883, 2012.

[16] G. R. Liu and S. S. Quek, "A non-reflecting boundary for analyzing wave propagation using the finite element method," *Fn. Elem. in Anal. Des.*, vol. 39, pp.403–417, 2003.

[17] M. Drozdz, L. Moreau, M. Castaings, M. J. S. Lowe and P. Cawley, "Efficient numerical modelling of absorbing regions for boundaries of guided waves problems," *Rev. of Prog. Quant. Nondest. Eval.*, Vol. 25, pp.126–133, 2006.

[18] A. Velichko and P. D. Wilcox, "A generalized approach for efficient finite element modeling of elastodynamic scattering in two and three dimensions," *J. Aoust. Soc. Am.*, vol. 128, pp.1004–1014, 2010.

[19] ABAQUS,ABAQUS Analysis User's Manual, Version 6.9, Dassault Systemes, 2009.

[20] A. Velichko and P. D. Wilcox, "A geralized approach for efficient finite elment modeling of elastodynamic scattering intwo and three dimensions," *J. Acoust. Soc. Am.* Vol. 128, pp.1004–1014, 2010.

[21] M. J. S. Lowe, P. Cawley, J. Y. Kao and O. Diligent, "The low frequency reflection characterstics of the fundamental antisymmetric Lamb wave a0 from a rectangular notch in a plate," *J. Acoust. Soc. Am.*, vol. 112, pp.2612–2622, 2002.

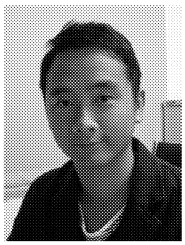

Ching-Tai Ng was born in Hong Kong, China in 1983. He received B.Eng. and M.Phil. degrees from City University of Hong Kong, in 2005 and 2007, respectively, and then Ph.D. degree from The University of Queensland, Australia, in 2011. He joined The University of Adelaide as a Lecturer (Level B) in 2011. His research interests include structural health monitoring, guided wave non-destructive evaluation, system identification, engineering reliability and risk analysis and composite materials with applications to different engineering areas.